Biochemical and Biophysical Research Communications 452 (2014) 940–944

Contents lists available at ScienceDirect

Biochemical and Biophysical Research Communications

journal homepage: www.elsevier.com/locate/ybbrc

A unique mechanism of curcumin inhibition on F_1 ATPase

Mizuki Sekiya [a], Ryosuke Hisasaka [a], Atsuko Iwamoto-Kihara [b], Masamitsu Futai [a], Mayumi Nakanishi-Matsui [a,*]

[a] Department of Biochemistry, Faculty of Pharmaceutical Sciences, Iwate Medical University, and Futai Special Laboratory, Yahaba, Iwate 028-3694, Japan
[b] Department of Bioscience, Nagahama Institute of Bioscience and Technology, Nagahama, Shiga 526-0829, Japan

ARTICLE INFO

Article history:
Received 29 August 2014
Available online 16 September 2014

Keywords:
ATP synthase
F_1 ATPase
ATPase rotational catalysis
Curcumin
Quercetin
Piceatannol

ABSTRACT

ATP synthase (F-ATPase) function depends upon catalytic and rotation cycles of the F_1 sector. Previously, we found that F_1 ATPase activity is inhibited by the dietary polyphenols, curcumin, quercetin, and piceatannol, but that the inhibitory kinetics of curcumin differs from that of the other two polyphenols (Sekiya et al., 2012, 2014). In the present study, we analyzed *Escherichia coli* F_1 ATPase rotational catalysis to identify differences in the inhibitory mechanism of curcumin versus quercetin and piceatannol. These compounds did not affect the 120° rotation step for ATP binding and ADP release, though they significantly increased the catalytic dwell duration for ATP hydrolysis. Analysis of wild-type F_1 and a mutant lacking part of the piceatannol binding site (γΔ277–286) indicates that curcumin binds to F_1 differently from piceatannol and quercetin. The unique inhibitory mechanism of curcumin is also suggested from its effect on F_1 mutants with defective β–γ subunit interactions (γMet23 to Lys) or β conformational changes (βSer174 to Phe). These results confirm that smooth interaction between each β subunit and entire γ subunit in F_1 is pertinent for rotational catalysis.

1. Introduction

ATP synthase (F-ATPase), found in membranes of bacteria, chloroplasts, and mitochondria, plays critical roles in energy transduction (for reviews, see Refs. [1–6]). F-ATPase consists of the catalytic F_1 sector ($\alpha_3\beta_3\gamma\delta\varepsilon$) and the trans-membrane proton pathway, the F_o sector (ab_2c_{10}). The rotation of a subunit complex (γ, ε, and *c*-ring) against stator subunits couples ATP synthesis or hydrolysis in F_1 with proton translocation through F_o. Crystal structures of bovine F_1 [7] indicate that the β subunit transitions sequentially through three distinct conformations, β_{TP}, β_{DP}, and β_E (β catalytic sites with bound ATP, ADP, or no nucleotide, respectively), consistent with cooperative catalysis. In ATP synthesis, the empty β subunit binds to ADP, passing from β_E to β_{DP} and then to β_{TP}; in hydrolysis, the conformations progress from β_E to β_{TP} and then to β_{DP}. The *Escherichia coli* F_1 crystal structure further supports this mechanism [8].

Direct observation of ATP hydrolysis-dependent single molecule rotation has contributed to our understanding of rotational catalysis [9–13], in which changes in the β subunit structure are pertinent for efficient energy coupling between catalysis and proton transport. The γ subunit continuously rotates within the $\alpha_3\beta_3$ hexamer, advancing in 120° steps [14–15]. During hydrolysis, upon ATP binding to β_E, the γ subunit mechanically rotates 80° and enters a pause called catalytic dwell when ATP is reversibly hydrolyzed to ADP and P_i in β_{TP}. Following hydrolysis, the enzyme passes through a rate-limiting transition state, triggering the 40° revolution in which ADP and P_i dissociate from the β_{DP} site and restore the β_E conformation [16]. The catalytic dwell between the 80° and 40° revolutions is unaffected by ATP concentration and can be resolved in single molecule observations under V_{max} conditions with saturating ATP [17]. By contrast, the ATP waiting dwell (time for ATP binding to β_E) is very short (<0.1 ms) and cannot be resolved, even with faster time resolution [18]. Our extensive studies of *E. coli* F-ATPase kinetics reveal stochastic fluctuation of rotation with a flat catalytic energy pathway [17,19].

Previously, we found that three polyphenols, piceatannol, quercetin, and curcumin (Fig. 1), lower the V_{max} of bulk phase F_1 ATPase activity [20,21]. However, while piceatannol and quercetin significantly increase *km*, curcumin has no effect on *km*, implicating a different inhibitory mechanism from that of the other two polyphenols [21]. Single molecule studies reveal that piceatannol inhibits F_1 ATPase activity by increasing the activation energy of the rate-limiting transition state and lowering the rotation rate [20]. Because analogous studies have not been performed for curcumin, it is of interest to know whether curcumin affects rotational

Abbreviations: P_i, inorganic phosphate; rps, revolutions per second.

* Corresponding author. Fax: +81 19 698 1843.
E-mail address: nakanim@iwate-med.ac.jp (M. Nakanishi-Matsui).

http://dx.doi.org/10.1016/j.bbrc.2014.09.027
0006-291X/

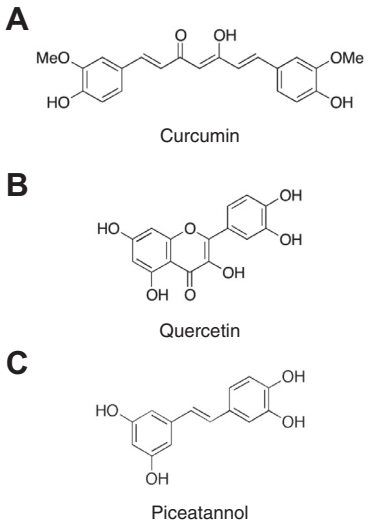

Fig. 1. Chemical structures of curcumin, quercetin, and piceatannol. The structures of curcumin (1*E*,6*E*)-1,7-bis(4-hydroxy-3-methoxyphenyl)-1,6-heptadiene-3,5-dione (A), quercetin (2-(3,4-dihydroxyphenyl)-3,5,7-trihydroxy-4*H*-chromen-4-one) (B), and piceatannol (*trans*-3,3′,4′,5-tetrahydroxystilbene) (C) are shown.

catalysis by a similar mechanism to that of the other polyphenols. Here, we investigated the effects of polyphenols on the rotation of the γ subunit and found that the mechanism of curcumin inhibition is different from that of piceatannol or quercetin. Thus, studies of polyphenol mediated inhibition may contribute to our mechanistic understanding of F-ATPase rotational catalysis.

2. Materials and methods

2.1. Preparation and materials

A recombinant plasmid carrying all F-ATPase genes was used as the wild-type throughout this study [22]; for the rotation assay, modifications were made in the γ (γS193C and γK108C) and α (six His residues connected to amino terminus) subunits [19]. βS174F and γM23K mutations were introduced as previously described [23,24]. Similarly, a stop codon was introduced at Thr277 of the γ subunit gene. The *E. coli* strain, DK8, harboring the recombinant plasmid with wild-type or mutant F-ATPase genes was grown with glycerol as the sole carbon source. Membranes were prepared by disrupting cells in a French Press, and an apparently homogenous F_1 sector was prepared as previously described [22]. Curcumin, quercetin, and piceatannol were purchased from Enzo Life Sciences (Farmingdale, NY). Other materials used were of the highest grade commercially available.

2.2. Assay procedures

ATPase activity and protein concentrations were assayed as described previously [21]. For the rotation assay, a gold bead (British Bio Cell International, 60 nm diameter) was attached to the γ subunit of F_1, which was immobilized on a glass surface. Rotation was observed by dark-field microscopy under laser light illumination [19], and the results were analyzed with modified MATLAB (The Mathworks, Inc.) and Image J (NIH, USA).

3. Results and discussion

3.1. Inhibitory effects of polyphenols on F_1 ATPase γ subunit rotation

For analyzing rotation, the γ subunit was attached to a gold bead, which was small enough (60 nm diameter) to negate the effects of viscous drag [19]. We examined rotation in the presence of 30 μM curcumin, 100 μM quercetin, or 200 μM piceatannol. At these concentrations, more than 90% of F_1 should be bound to each of the polyphenols because the K_i values are 1.0, 8.0, and 20 μM, respectively [20,21]. Time courses (2 s) of continuous rotation were used to monitor the rotation rates, which were obtained from reciprocals of the average time required for a 360° revolution. The wild-type control rate without inhibitors was 300 rps (revolutions per s) (Table 1); this slightly-lower control rate compared to our previous results may be due to the presence of DMSO and to a different F_1 preparation. By contrast, the average rates in the presence of curcumin, quercetin, and piceatannol were 98, 213, and 102 rps, respectively (Table 1 and Fig. 2A), clearly indicating that these polyphenols lowered the rotation rates.

Under V_{max} conditions (2 mM ATP and 2 mM $MgCl_2$), the beads rotate in successive 120° steps, including a short catalytic dwell and a 120° rotation step of ~0.4 and ~0.7 ms, respectively (Fig. 2B) [17]. Expanded time courses for randomly selected beads showed that polyphenols extended the catalytic dwell duration, which includes the reversible ATP hydrolysis/synthesis step and the rate-limiting transition state that triggers subsequent rotation (Fig. 2C). But these compounds had essentially no effect on the 120° rotation step (Fig. 2C), which includes ADP and P_i release, as well as ATP binding.

The average catalytic dwell in the presence of polyphenols ranged from 0.8 to 3.0 ms, 2.4- to 8.0-fold longer than in the absence of the inhibitor, 0.3 ms (Fig. 2D: closed bars); the longest duration was with curcumin (8-fold longer). By contrast, polyphenols only slightly affected the time for the 120° rotation step (Fig. 2D: open bars).

3.2. Inhibitory mechanism on the catalytic dwell with different polyphenols

Crystal structures of bovine F_1 (24) show that piceatannol and quercetin bind to a pocket formed by the γ subunit carboxyl terminus and amino acid residues of the subunit conformers, α_{DP}, α_{TP}, and β_{TP} [25] (Fig. 3A). Because the bovine [7] and *E. coli* [8] F_1 structures are highly similar, we inferred that the same binding site is present in both species. Following this assumption, piceatannol and quercetin should interact with the *E. coli* γ subunit Ala270, Thr273, Gln274, Thr277, and Glu278 (Fig. 3B).

To determine if curcumin also binds to the γ subunit carboxyl terminal region, we performed rotation assays to measure the *E. coli* F_1 catalytic dwell duration with either or both polyphenols. Compared to the untreated control, upon the addition of saturating concentrations of piceatannol or quercetin, the dwell durations were increased 6.7- or 2.4-fold, respectively (Fig. 3C:+Pic and + Que). However, in the presence of both piceatannol and

Table 1
Rotation rates of wild-type and mutant F_1 sectors in the presence of polyphenols. F_1 γ subunit rotations were followed in the presence of 30 μM curcumin (+Cur), 100 μM quercetin (+Que), or 200 μM piceatannol (+Pic). Because the K_i values for curcumin, quercetin, and piceatannol are 1.0, 8.0, and 20 μM, respectively, at the concentrations shown above, the F_1 sectors should be more than 90% bound to polyphenols [20,21]. Rotation rates were obtained from the reciprocal of the average time required for a 360° revolution.

Mutations in the γ or β subunits	Rotation rate (revolutions/s, rps)			
	None	+Cur	+Pic	+Que
Wild-type	300	98	102	213
γΔ277–283	281	89	181	255
γM23K	160	65	33	NT*
βS174F	75	26	41	NT*

* Not tested.

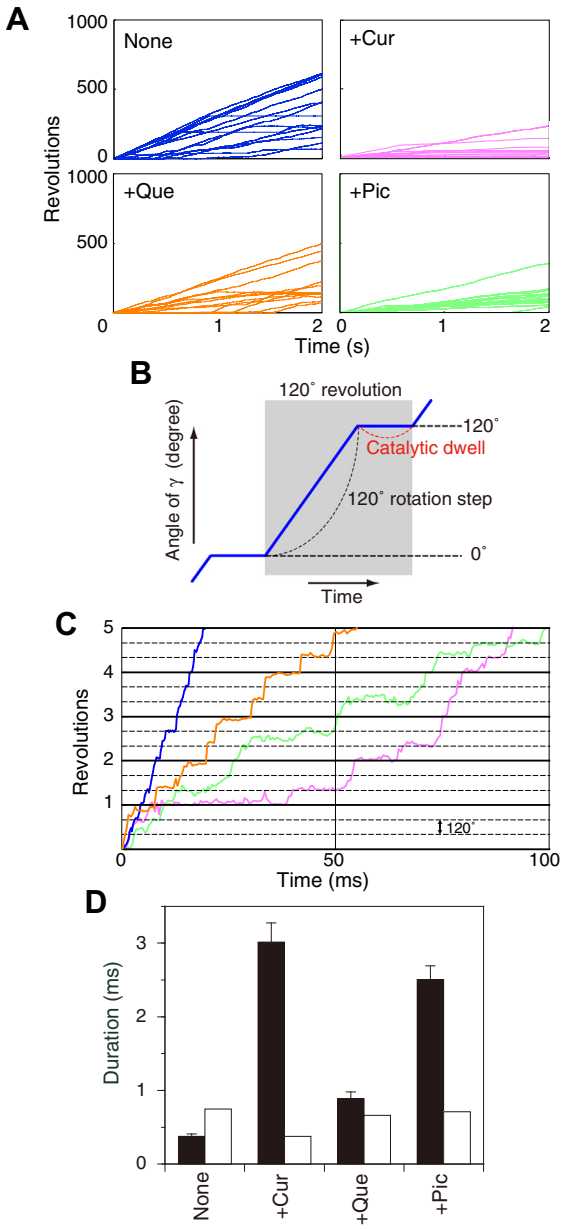

Fig. 2. Effects of polyphenols on γ subunit rotational catalysis. (A) Beads connected to individual γ subunits were selected at random and followed for 2 s to measure rotation rates in the presence of 30 μM curcumin (+Cur, magenta), 100 μM quercetin (+Que, orange), or 200 μM piceatannol (+Pic, green). The control condition (None, blue), 0.5% dimethyl sulfoxide (DMSO) was the vehicle for polyphenol addition. (B) A schematic representation of F_1 rotational catalysis under V_{max} conditions. A complete 120° revolution is shown, including the catalytic dwell and the 120° rotation step. (C) Expanded time courses are shown for rotations of randomly selected beads connected to individual γ subunits, in the presence or absence of polyphenols as indicated by the trace colors shown in A. (D) Effects of polyphenols on the duration of the catalytic dwell and the 120° rotation step. Average durations of the catalytic dwell (closed bars) and the 120° rotation step (open bars) are shown. Results are shown with standard error (SE). Duration time for the 120° rotation step was determined statistically by subtracting the duration of catalytic dwell from that of the complete 120° revolution.

quercetin, the catalytic dwell duration was increased 6.2-fold (Fig. 3C: Que + Pic), essentially the same as with piceatannol alone (Fig. 3C:+Pic), indicating no combined effect of the two polyphenols. These results support the conclusion that piceatannol and quercetin share mutual inhibitory binding sites on *E. coli* F_1 [25].

On the other hand, relative to the control condition, the addition of curcumin increased the catalytic dwell duration by 8.0-fold (Fig. 3C: Cur), and the inclusion of quercetin further increased this duration to 11-fold (Fig. 3C: Cur + Que), demonstrating a combined effect of quercetin and curcumin. The catalytic dwell durations for curcumin (3.0 ms) and quercetin (0.8 ms) represent increases of 2.6 and 0.5 ms above the control, respectively. The dwell duration in the combined presence of both compounds (4.0 ms) was 3.6 ms longer than that of the control and very close to the predicted value for an additive effect (2.6 ms + 0.5 ms = 3.1 ms ≈ 3.6 ms).

Curcumin and piceatannol also showed a combined effect with respect to catalytic dwell duration. The durations with curcumin (3.0 ms) or piceatannol (2.5 ms) alone were 2.6 ms or 2.1 ms longer than the untreated control duration, respectively (Fig. 3C:+Cur and +Pic); simultaneous inclusion of both compounds increased the dwell duration (10.2 ms) to 9.9 ms above the control (Fig. 3C: Cur + Pic), indicating a positive interaction (2.6 ms + 2.1 ms = 4.7 ms < 9.9 ms). The combined effects of curcumin with piceatannol and quercetin confirm that curcumin affects the catalytic dwell differently from the other polyphenols.

To further query this mechanism, we truncated the γ subunit between Thr277 and the carboxyl terminus (Val286) (Fig. 3B): the truncated mutant showed essentially the same average rotation rate (281 rps) as the wild-type F_1 but with varied effects of the polyphenols. For the γΔ277–283 mutant F_1, measured rotation rates in the presence of curcumin, quercetin, and piceatannol were 89, 255, and 181 rps, respectively (Table 1, γΔ277–283). To compare the effects of polyphenols on the mutant versus wild-type F_1 constructs, relative values were calculated from the rotation rates shown in Table 1. Relative to the untreated condition, in the presence of piceatannol or quercetin, rotation rates were significantly higher for the truncation mutant (64% or 90% of control, respectively) versus wild-type F_1 (34% and 71% of control, respectively). By contrast, the effect of curcumin on the rotation rate was essentially the same for both mutant and wild-type F_1 (32% versus 33% of control, respectively).

Similar to their effect on rotation rate, polyphenols also affected the catalytic dwell of the mutant F_1 (Fig. 3D, γΔ277–286); the dwell durations with piceatannol and quercetin were 1.1 and 0.8 ms, respectively, which is slightly longer than in the untreated control condition (0.5 ms). On the other hand, the dwell duration with curcumin was 3.9 ms (an 8.3-fold increase over the control), which is essentially an identical increase to that observed for wild-type F_1 (Fig. 3C and D:+Cur). These results indicate that the γ subunit carboxyl terminus is not required for curcumin binding, as it is for other polyphenols.

3.3. Effects of polyphenols on mutant F_1 with defects in β–γ interaction or conformational changes of the β hinge region

Previously, we showed that interactions between the γ and the three β subunits greatly influence rotational catalysis efficiency [17]. A mutation at γ subunit residue 23 (M23K) caused defective energy coupling, most likely via an added interaction between the γ rotor (mutant γLys23) and the β stator (βGlu381) [17]. Because both piceatannol and quercetin inhibit rotation by affecting the β–γ interaction, we were interested to study the effects on rotational catalysis of the F_1 γM23K mutant.

Consistent with our previous results, the average rotation rate of the γM23K mutant F_1 was about half that of the wild-type (Table 1) [17]. Correspondingly, the mutant had a longer catalytic dwell duration of 1.6 ms, increased by 1.2 ms (4.2-fold) over the wild-type (Fig. 3C: None; Fig. 4A: None, closed bar). Based on a catalytic dwell duration of 3.0 ms for wild-type F_1 in the presence of curcumin (Fig. 3C:+Cur), we expected the corresponding duration to be near 4.2 ms (3.0 ms + 1.2 ms = 4.2 ms) for M23K F_1, reflecting

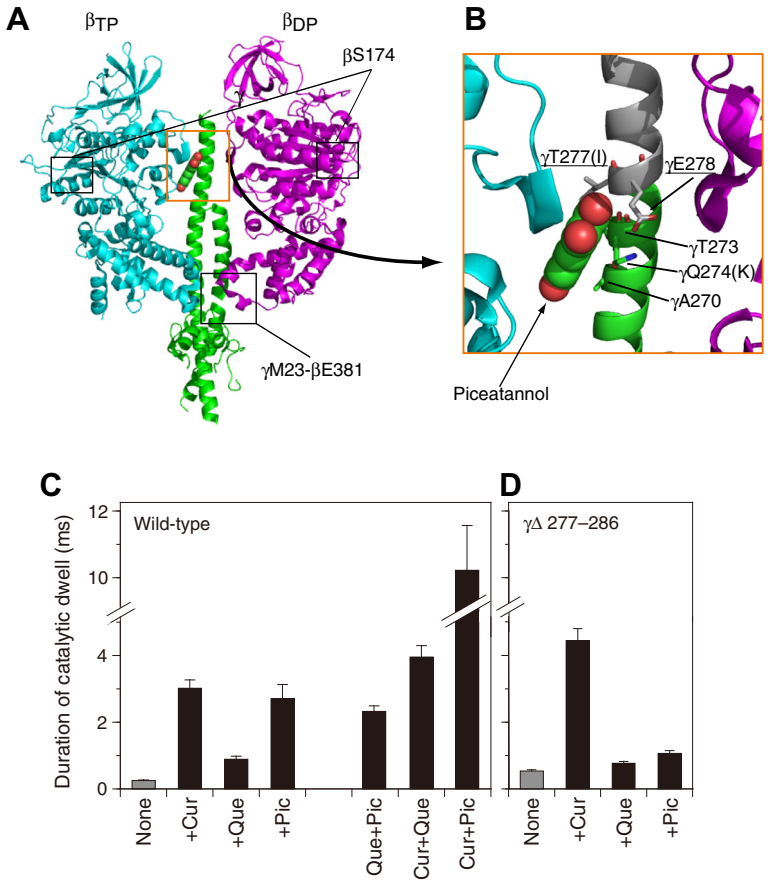

Fig. 3. Polyphenol binding sites on the F_1 ATPase. (A) Piceatannol binding site and amino acid residues featured in this study. A three-dimensional structure model shows bovine β subunits bound to ATP (β_{TP}; cyan) and ADP (β_{DP}; magenta) in their positions relative to the γ subunit (green). Amino acid residue positions analogous to *E. coli* βS174 and γM23–βE381 interacting site are also shown. (B) Expanded image of piceatannol binding site. Residues corresponding to those forming the piceatannol binding site of the *E. coli* γ subunit are shown in the bovine γ subunit structure (based on the model by Gledhill et al. [25]). Numbering is shown for residues at corresponding positions on the *E. coli* γ subunit in which γQ274 and γT277 correspond to bovine Lys and Ile residues, respectively. The *E. coli* γΔ277–286 mutant lacks the helix between Thr277 and the carboxyl terminus (Val286) (shown in gray) of the wild-type γ subunit. (C) Effects of polyphenols on catalytic dwell. F_1 was incubated with 30 μM curcumin (+Cur), 100 μM quercetin (+Que), or 200 μM piceatannol (+Pic) for 60 min. Combinations of these compounds were similarly tested (Que + Pic, Cur + Que, and Cur + Pic). The rotations of randomly selected beads were followed for time courses of 2 s, and catalytic dwell durations are shown as mean ± SE. Wild-type dwell duration without polyphenol addition (None) is cited from Fig. 2D for comparison. (D) Effects of polyphenols on the rotation of a γ subunit mutant lacking the carboxyl terminus. Gold beads were attached to the γ subunit lacking carboxyl terminus (γΔ277–286), and rotations were followed for randomly selected beads in the presence of 30 μM curcumin (+Cur), 100 μM quercetin (+Que), or 200 μM piceatannol (+Pic). Catalytic dwell durations are shown as mean ± SE.

separate effects of the mutation and curcumin on the catalytic dwell (Fig. 4A:+Cur, gray bar). Consistent with our prediction (4.2 ms), the catalytic dwell was 4.4 ms for γM23K F_1 in the presence of curcumin (Fig. 4A:+Cur, closed bar). These results suggest that the γM23K mutation and curcumin affect the catalytic dwell via independent mechanisms.

As described above, with piceatannol, the catalytic dwell duration of wild-type F_1 was 2.5 ms (Fig. 3C:+Pic). By contrast, the corresponding dwell of γM23K F_1 was 12.6 ms, almost 3-fold higher than that expected for separate additive effects of the mutation and piceatannol (2.5 ms + 1.2 ms = 3.6 ms) (Fig. 4A:+Pic, compare closed and gray bars). These results suggest that piceatannol acts synergistically with the γM23K mutation to increase the catalytic dwell duration; according to transition state theory, this indicates that piceatannol and the γM23K mutation affect the same reaction phase. These results are consistent with our earlier report that both piceatannol and γM23K increase the activation energy required to overcome the β–γ interaction [20].

Previously, we suggested that nucleotide binding dramatically changes the conformation of the β hinge domain near the catalytic site (βPhe148–βGly186; the β-sheet 4/loop/α-helix B/P-loop domain) and that Ser174 to Phe substitution (βS174F) in β-sheet 4 perturbs the rotation of the F_1 γ subunit [15,23]. Homology modeling revealed that Phe174 forms a hydrophobic network with Met159, Ile163, and Ala167 in nucleotide-bound β subunits, which significantly affects β subunit conformation (Fig. 3A) [4,26].

Consistent with our previous results, the βS174F mutant average rotation rate was about 1/4 that of wild-type F_1 (Table 1) [15]. Correspondingly, the catalytic dwell duration was increased by 3.7 ms (4.2-fold) over the wild-type (Fig. 3C: None; Fig. 4B: None, closed bar). With inclusion of piceatannol, the dwell duration increased to 5.2 ms (Fig. 4B:+Pic, closed bar), essentially the same value as that expected for the individual additive effects of the βS174F mutation and piceatannol (Fig. 4B:+Pic, gray bar), suggesting that the two effects are independent. For the βS174F mutant in the presence of curcumin, the dwell duration was 24.0 ms, which is 4-fold higher than the predicted value of 6.7 ms based on separate additive contributions of the βS174F mutation (3.7 ms) and curcumin (3.0 ms) (Fig. 4B:+Cur, compare closed and gray bars). This effect of curcumin on the catalytic dwell of βS174F F_1 is different from that of curcumin on γM23K

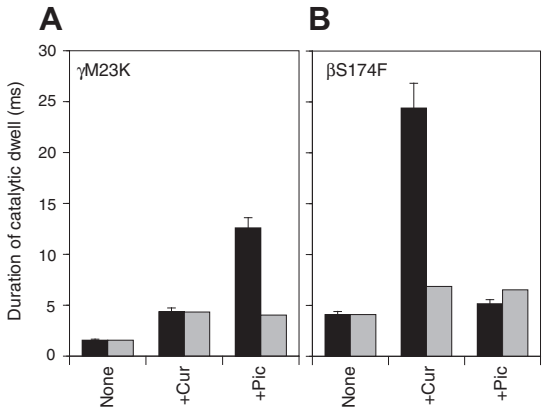

Fig. 4. Effects of polyphenols on the catalytic dwell duration for γM23K and βS174F mutants. (A) Effects of polyphenols on the catalytic dwell of the γM23K mutant. The mutant F_1 sector was incubated with curcumin (+Cur) or piceatannol (+Pic) for 60 min, and rotations were followed over a 2 s interval. Catalytic dwell durations for the γM23K mutant are shown as mean ± SE (closed bars). Gray bars indicate hypothetical catalytic dwell durations estimated from the combined sum of the individual effects of mutations or polyphenols alone. (B) Effects of polyphenols on the catalytic dwell of the βS174F mutant. The βS174F mutant F_1 sectors were incubated with curcumin (+Cur) or piceatannol (+Pic), and rotations were followed over a 2 s interval. Catalytic dwell durations of the mutant F_1 sector are shown as mean ± SE.

F_1. The apparent synergy may be due to a functional interaction between the curcumin binding site and the βS174F mutant catalytic site.

In this study, our results suggest that curcumin inhibit F_1 ATPase activity by disrupting β subunit catalytic site conformational transitions and extending catalytic dwell. We found that the curcumin inhibitory mechanism is different from that of other polyphenols. Combined studies of curcumin and F_1 mutants also confirmed our prior notion that β–γ interaction and β conformation change are pertinent for rotational catalysis [15,17].

Elucidating the curcumin inhibitory mechanism provides important clues for understanding rotational catalysis. In addition, polyphenols could be important seed compounds for drug development targeting bacterial ATP synthase [21].

Acknowledgments

We are grateful to Ms. Eri Nishiyama, Ms. Shio Yano, and Mr. Shusei Yoshida for their expert technical assistance. This work was supported by JSPS KAKENHI Grant Number 24790048.

References

[1] P.D. Boyer, The ATP synthase – a splendid molecular machine, Annu. Rev. Biochem. 66 (1997) 717–749.
[2] D. Stock, A.G.W. Leslie, J.E. Walker, Molecular architecture of the rotary motor in ATP synthase, Science 286 (1999) 1700–1705.
[3] R.H. Fillingame, C.M. Angevine, O.Y. Dmitriev, Mechanics of coupling proton movements to *c*-ring rotation in ATP synthase, FEBS Lett. 555 (2003) 29–34.
[4] M. Nakanishi-Matsui, M. Sekiya, R.K. Nakamoto, M. Futai, The mechanism of rotating proton pumping ATPases, Biochim. Biophys. Acta 1797 (2010) 1343–1352.
[5] M. Futai, M. Nakanishi-Matsui, H. Okamoto, M. Sekiya, R.K. Nakamoto, Rotational catalysis in proton pumping ATPases: from *E. coli* F-ATPase to mammalian V-ATPase, Biochim. Biophys. Acta 2012 (1817) 1711–1721.
[6] M. Nakanishi-Matsui, M. Sekiya, M. Futai, Rotating proton pumping ATPases: subunit/subunit interactions and thermodynamics, IUBMB Life 65 (2013) 247–254.
[7] J.P. Abrahams, A.G. Leslie, R. Lutter, J.E. Walker, Structure at 2.8 Å resolution of F_1-ATPase from bovine heart mitochondria, Nature 370 (1994) 621–628.
[8] A.C. Hausrath, R.A. Capaldi, B.W. Matthews, The conformation of the ε- and γ-subunits within the *Escherichia coli* F_1 ATPase, J. Biol. Chem. 276 (2001) 47227–47232.
[9] H. Noji, R. Yasuda, M. Yoshida, K. Kinosita, Direct observation of the rotation of F_1-ATPase, Nature 386 (1997) 299–302.
[10] H. Omote, N. Sambonmatsu, K. Saito, Y. Sambongi, A. Iwamoto-Kihara, T. Yanagida, Y. Wada, M. Futai, The γ-subunit rotation and torque generation in F_1-ATPase from wild-type or uncoupled mutant *Escherichia coli*, Proc. Natl. Acad. Sci. U.S.A. 96 (1999) 7780–7784.
[11] Y. Sambongi, Y. Iko, M. Tanabe, H. Omote, A. Iwamoto-Kihara, I. Ueda, T. Yanagida, Y. Wada, M. Futai, Mechanical rotation of the *c* subunit oligomer in ATP synthase (F_oF_1): direct observation, Science 286 (1999) 1722–1724.
[12] K. Nishio, A. Iwamoto-Kihara, A. Yamamoto, Y. Wada, M. Futai, Subunit rotation of ATP synthase embedded in membranes: a or β subunit rotation relative to the c subunit ring, Proc. Natl. Acad. Sci. U.S.A. 99 (2002) 13448–13452.
[13] M. Diez, B. Zimmermann, M. Börsch, M. König, E. Schweinberger, S. Steigmiller, R. Reuter, S. Felekyan, V. Kudryavtsev, C.A. Seidel, P. Gräber, Proton-powered subunit rotation in single membrane-bound F_oF_1-ATP synthase, Nat. Struct. Mol. Biol. 11 (2004) 135–141.
[14] K. Adachi, R. Yasuda, H. Noji, H. Itoh, Y. Harada, M. Yoshida, K. Kinosita Jr., Stepping rotation of F_1-ATPase visualized through angle-resolved single-fluorophore imaging, Proc. Natl. Acad. Sci. U.S.A. 97 (2000) 7243–7247.
[15] M. Nakanishi-Matsui, S. Kashiwagi, T. Ubukata, A. Iwamoto-Kihara, Y. Wada, M. Futai, Rotational catalysis of *Escherichia coli* ATP synthase F_1 sector. Stochastic fluctuation and a key domain of the β subunit, J. Biol. Chem. 282 (2007) 20698–20704.
[16] J.A. Scanlon, M.K. Al-Shawi, P.N. Le, R.K. Nakamoto, Determination of the partial reactions of rotational catalysis in F_1-ATPase, Biochemistry 46 (2007) 8785–8797.
[17] M. Sekiya, R.K. Nakamoto, M.K. Al-Shawi, M. Nakanishi-Matsui, M. Futai, Temperature dependence of single molecule rotation of the *Escherichia coli* ATP synthase F_1 sector reveals the importance of γ-β subunit interactions in the catalytic dwell, J. Biol. Chem. 284 (2009) 22401–22410.
[18] R. Yasuda, H. Noji, M. Yoshida, K. Kinosita, H. Itoh, Resolution of distinct rotational substeps by submillisecond kinetic analysis of F_1-ATPase, Nature 410 (2001) 898–904.
[19] M. Nakanishi-Matsui, S. Kashiwagi, H. Hosokawa, D.J. Cipriano, S.D. Dunn, Y. Wada, M. Futai, Stochastic high-speed rotation of *Escherichia coli* ATP synthase F_1 sector: the ε subunit-sensitive rotation, J. Biol. Chem. 281 (2006) 4126–4131.
[20] M. Sekiya, R.K. Nakamoto, M. Nakanishi-Matsui, M. Futai, Binding of phytopolyphenol piceatannol disrupts β/γ subunit interactions and rate-limiting step of steady-state rotational catalysis in *Escherichia coli* F_1-ATPase, J. Biol. Chem. 287 (2012) 22771–22780.
[21] M. Sekiya, E. Chiba, M. Satoh, H. Yamakoshi, Y. Iwabuchi, M. Futai, M. Nakanishi-Matsui, Strong inhibitory effects of curcumin and its demethoxy analog on *Escherichia coli* ATP synthase F_1 sector, Int. J. Biol. Macromol. 70C (2014) 241–245.
[22] Y. Moriyama, A. Iwamoto, H. Hanada, M. Maeda, M. Futai, One-step purification of *Escherichia coli* H^+-ATPase (F_oF_1) and its reconstitution into liposomes with neurotransmitter transporters, J. Biol. Chem. 266 (1991) 22141–22146.
[23] A. Iwamoto, H. Omote, H. Hanada, N. Tomioka, A. Itai, M. Maeda, M. Futai, Mutations in Ser174 and the glycine-rich sequence (Gly149, Gly150, and Thr156) in the β subunit of *Escherichia coli* H^+-ATPase, J. Biol. Chem. 266 (1991) 16350–16355.
[24] K. Shin, R.K. Nakamoto, M. Maeda, M. Futai, F_oF_1-ATPase γ subunit mutations perturb the coupling between catalysis and transport, J. Biol. Chem. 267 (1992) 20835–20839.
[25] J.R. Gledhill, M.G. Montgomery, A.G. Leslie, J.E. Walker, Mechanism of inhibition of bovine F_1-ATPase by resveratrol and related polyphenols, Proc. Natl. Acad. Sci. U.S.A. 104 (2007) 13632–13637.
[26] S. Kashiwagi, A. Iwamoto-Kihara, M. Kojima, T. Nonaka, M. Futai, M. Nakanishi-Matsui, Effects of mutations in the β subunit hinge domain on ATP synthase F_1 sector rotation: interaction between Ser 174 and Ile 163, Biochem. Biophys. Res. Commun. 365 (2008) 227–231.